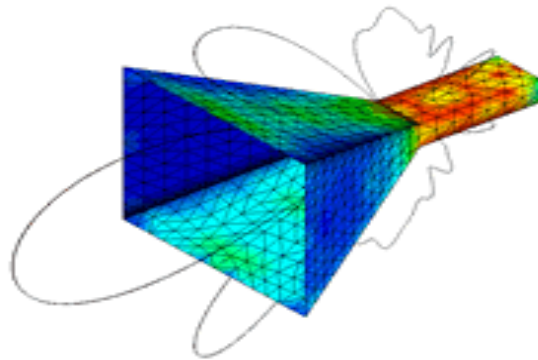


Microwave Horn Antenna Design and Test System

EE198B: Senior Design Project II
San Jose State University
Fall 2003



Presented by:

Vishal Ohri

Ozair Amin

Hiruy Gebremariam

Benjamin Dubois

Table of Contents

- Abstract 2
- Introduction 3
- Background and Theory 4
- Basics of Antenna Patterns Measurements 5
- Results and Analysis 8
 - I Waveguide design and tuning 8
 - II Horn Antenna design 10
 - III Test Setup and Measurements 11
- Discussion 14
- Concluding Remarks 14
- Reference 15
- Appendix 16

Abstract

This paper is our report for our senior design project on Microwave Antenna Design and Test System. This project requires two primary areas of concern; a pyramidal horn antenna design and a test system that will determine the performance of our antenna. A brief theory on microwave horn antennas will be discussed along with the results of our design. Our results and analysis show that the project was within the scope of our ability to design and test the horn antennas.

Introduction

In today's technological society, wireless communication has become an increasingly important part of daily life. We have come to depend on our pagers, cellular phones, satellite dishes, radios, etc., usually without understanding how they work. The common element to all of these wireless systems, whether they transmit or receive, is the antenna. The antenna is responsible for coupling the RF energy from the transmission-line feed (guided) to free space (unguided), and vice versa. Antennas are characterized using several parameters, such as geometry, gain, beamwidth, side-lobe level, frequency of operation, efficiency, and polarization. Keeping this in mind for this senior design project we designed two microwave horn antennas and implement a test system that will test the performance of our antenna and the efficiency of our test system. This paper will address the theoretical and practical construction of a 2.4GHz horn antenna and methodology used in testing the antennas. The pyramidal horn antenna is part of the aperture antennas family that has a conical radiation pattern, linearly polarized and is ideal in high gain transmission and receiving, peer to peer communications, and as a dish feed.

Background and theory

Currently there are many companies developing microwave antennas and highly sophisticated test systems that range in the millions of dollars. Our aim is to build an affordable horn antenna, less than \$20, and an inexpensive antenna test system setup. Horn antennas are extremely popular in the microwave region (above 1 GHz). Horns provide high gain, low VSWR (with waveguide feeds), relatively wide bandwidth, and they are not difficult to make. There are three basic types of rectangular horns:

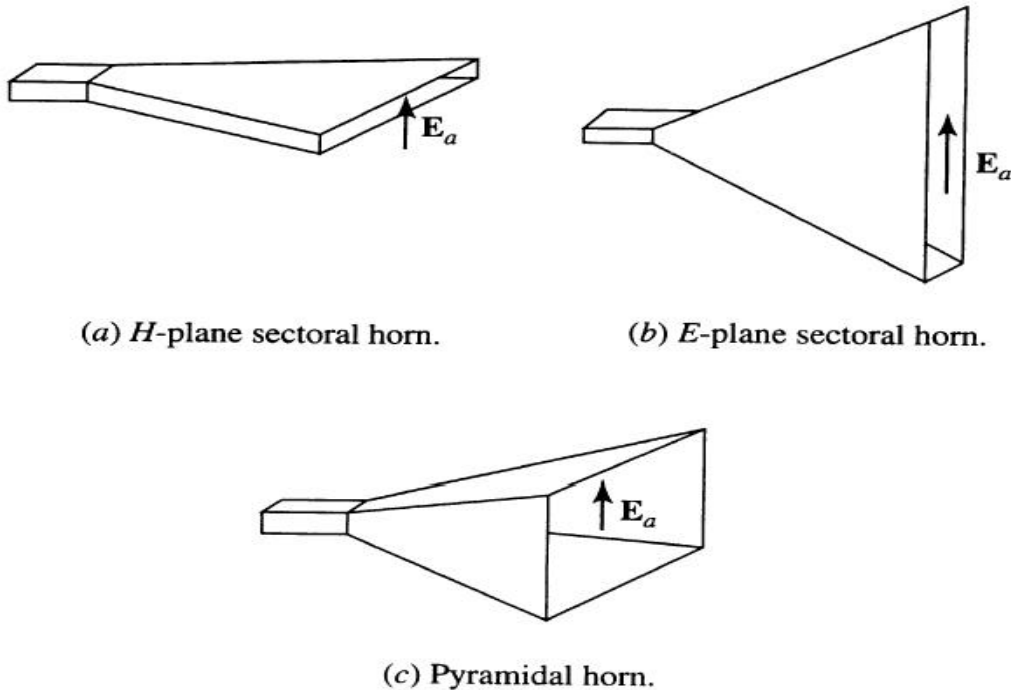


Figure 1: Basic types of horn antennas

We are concerned with the pyramidal horn antenna shown in Figure 1(c). The horns can be flared exponentially, too. This provides better matching in a broad frequency band, but is technologically more difficult and expensive. The rectangular horns are ideally suited for rectangular waveguide feeders. The horn acts as a gradual transition from a waveguide mode to a free-space mode of the EM wave. The open-ended waveguide will radiate, but not as effectively as the waveguide terminated by the horn antenna. The wave impedance inside the waveguide does not match that of the surrounding medium creating a mismatch at the open end of the waveguide. Thus, a portion of the outgoing wave is reflected back into the waveguide. The horn antenna acts as a matching network, with a gradual transition in the wave impedance from that of the waveguide to that of the surrounding medium. With a matched termination, the reflected wave is minimized and the radiated field is maximized. Designing the horn antenna is easy once we determine the dimensions of our horn antenna. There are many software programs available for download that can calculate the E-field and H-field dimensions of our horn for a given frequency (2.4GHz) and gain of about 19dB.

The horn antenna we design fit the following specification:

- 2.4 GHz (S-band)
- Beam width $\sim 17^\circ$
- ~ 19 dB gain
- Linearly polarized
- Return loss of > -10 dB (SWR $< 1.2:1$)
- WR430 Waveguide standard (4.30"X2.15")
- Waveguide to Coax adapter N-type connectors

Basics of Antenna Pattern Measurements

A general system designed for antenna measurements uses the following algorithm for performing a far-field antenna pattern measurement. An antenna under test (AUT) goes through all the desired angular configurations, while the AUT's response to RF stimulus (illuminated by a still source antenna) is being recorded. The plot of magnitude of the received signal versus angle displays the pattern directivity. As the process of measurement (rotating the AUT and recording the pattern) is usually done by the system, an operator has to set up (install/mount) the AUT and source antenna correctly. There are two major requirements to be satisfied: Realizing which plane (E or H) is to be used. This defines the placement of the AUT on the rotating table; Matching the polarization of AUT with the polarization of source antenna (if not measuring cross-polarization). The radiation pattern of an antenna describes its far field directional characteristics. When the antenna is transmitting the pattern indicates the relative power density radiated in different directions in the plane relative to the antenna principal direction of radiation ("bore-sight"). When receiving the pattern indicates the variation in the received signal level relative to bore-sight signal level as the antenna orientation is changed. Figure 2 shows a typical antenna radiation pattern.

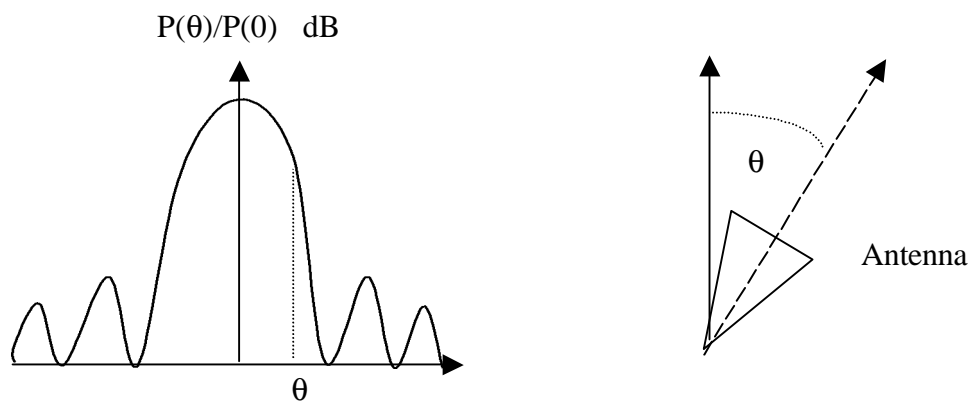


Figure 2: typical antenna radiation pattern

The radiation pattern can be measured in different spatial planes, principally the E and H planes as shown in figure 3 on the next page.

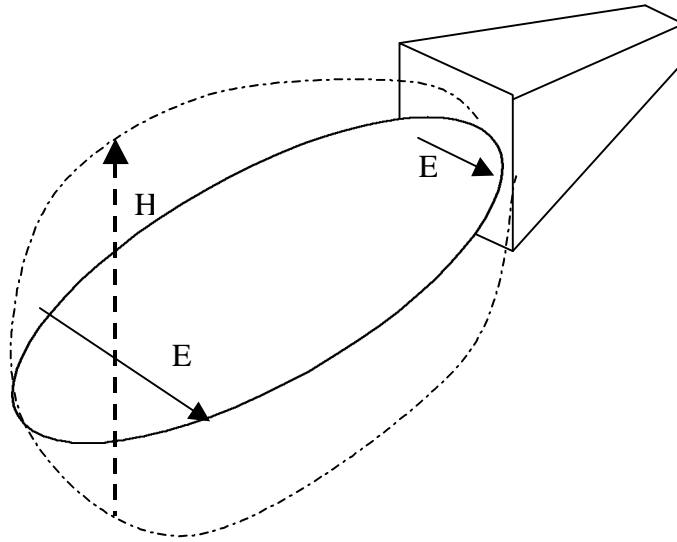


Figure 3: The E-field and H-field orientation of a horn antenna

Example (measuring pattern of a horn in the E-plane)

As the definition says, the E-plane is determined by the direction of the electrical field. In Figure 4, a horn antenna is fed by a rectangular waveguide, where the electrical field has only components parallel to the narrower sides. Thus, the field distribution in the horn antenna should be similar – parallel to the Y-axis. Under normal circumstances, the horn antenna has its maximum radiation in the Z-axis. These two directions (the direction of the electrical field and the direction of the maximum radiation) define the E-plane by the Y and Z axes (or the plane $x=0$). Thus, if the antenna must, can rotate an AUT in horizontal plane, then for measuring in the E-plane, the above-mentioned horn antenna must be mounted with its E-plane parallel to the plane of rotation (horizontal plane). This antenna mast (antenna tower) is placed inside an anechoic chamber. Through a window in one of the walls, a source antenna illuminates the AUT. The E-plane is parallel to the floor (horizontal plane), the source antenna must be polarized horizontally. For example: if a similar horn antenna is used for the source antenna, it must be placed the same way as the AUT (here – with the wider sides vertically).

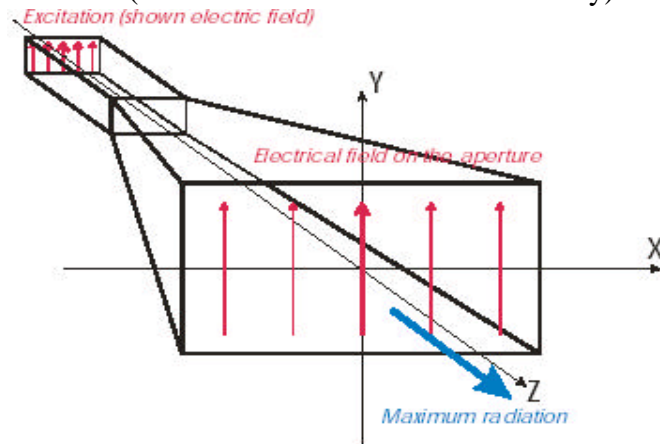
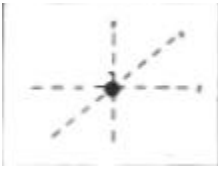

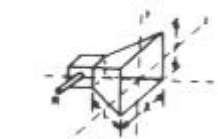



Figure 4: The E-field orientation

Antenna Chart

Name	Shape	Gain (over isotropic)	Beamwidth -3 dB	Radiation Pattern
Isotropic		0 dB	360	
Horn 3λ		15 dB	15	

Source: <http://www.tmeg.com/tutorials/antennas/antennas.htm>

Table 1: Gain, Beamwidth, and Radiation Pattern of horn relative to isotropic antenna

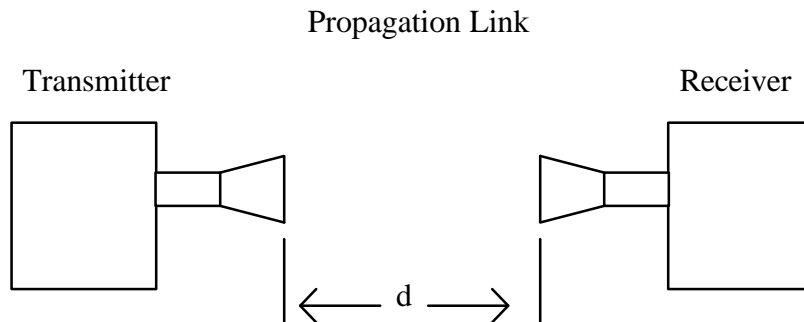


Figure 5: The antenna test system block diagram.

Ideally the antennas in the test system are put in a chamber (Faraday Cage) to eliminate any unwanted interference introduced by the inherent existence of EM waves in space. Since a perfect conductor is an idealization unavailable in nature, perfect Faraday cages do not exist. However, extremely good Faraday cages are constructed for electromagnetic experiments; they are commonly called "screen rooms." Early (and still common) screen rooms were made of copper mesh screen with a somewhat tighter mesh than typical aluminum window screen. Screen rooms are also made of welded sheet aluminum or sheet steel. For all screen rooms, special attention is given to electromagnetic sealing of closed doors and to metallic penetrations for power or communication. Screen rooms are typically designed to shield the enclosed volume from low-energy, high-frequency transmitted electromagnetic waves (e. g., AM/FM radio waves). Figure 6 shows our expected E-Field radiation pattern simulated using MatLab.

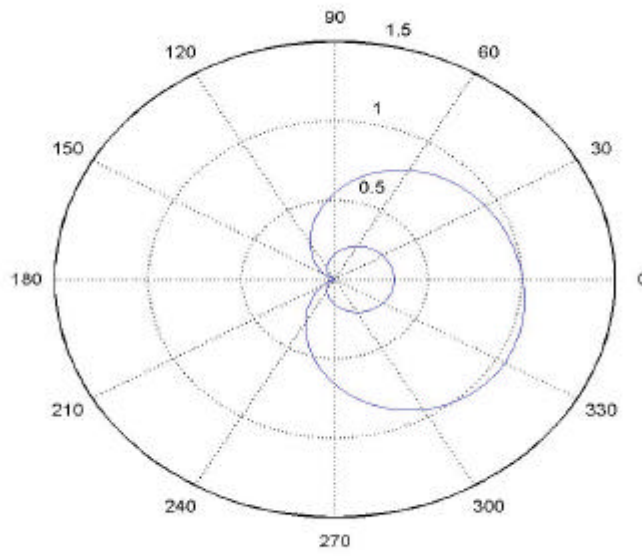
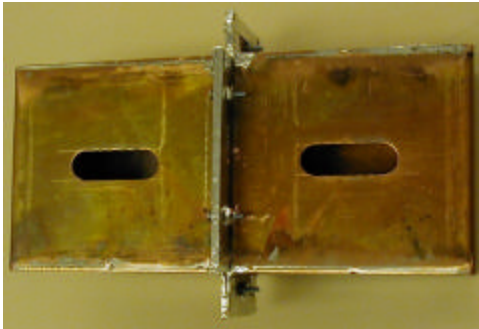


Figure 6: MatLab simulation of the E-field of a typical horn using the equations and code on Appendix.

Results and Analysis

I. Waveguide Design and tuning:



(a)



(b)

Picture 1: (a) top view of the WR430 waveguides attached together, (b) tuning screw under the waveguide.

We chose the standard waveguide (WR430), which operates in the frequency of our interest (2.4GHz). Once the two WR430 waveguides were built, we attached them facing each other with the slit open to allow us the freedom to move the N-connectors to the best location that have optimum S_{11} and S_{21} before attaching them to the horns. Picture 1 shows the setup for tuning the waveguides. After tuning the waveguides, we found out

that they had (1.70 -2.60) GHz, range and optimum location for the N-connectors was 1.23 inches from the back of the waveguide.



Picture 2: N-connector with a 1.18 inches of copper wire attached to it

Picture 2 shows the N-connector we used in our project. The length of the copper in the N connector was adjusted by trimming it little by little until the bandwidth of S_{11} was wide enough with an ideal gain of -20dB, and the transmission coefficient S_{21} was smooth between the 2.4GHz and 4.5GHz. Tuning the waveguide was the most important step in our testing procedure. Once we matched the two waveguides the horns was matched equivalently. A great deal of our time was spent trying to match the waveguides because we had to drill and open up more slit toward the back. Once we located the optimum point for the N-connector, we screwed five number 4-6 screws for tuning the waveguide even more. Picture 3 shows the S_{11} and S_{21} graphs displayed in the network analyzer while tuning the waveguide.



Picture 3: S_{11} and S_{21} measurements while tuning the waveguide

S_{11} measurement on picture 3 was improved to be -10.2dB at 2.4GHz. Ideally S_{11} is supposed to be -20dB. We spent days trying to tune the waveguides and obtain an S_{11} of -20dB, but it was impossible to reach that goal. The major reason was that the waveguides

were built in a machine shop where we did not have access to the equipment used to build the waveguides; hence the waveguides had manufacturing imperfections that made the tuning difficult. While doing the project, we found out that an ideal waveguide with an S_{11} of -20dB costs a little over \$1000. That is why for the price we paid for our waveguides, we were satisfied with what we got.

II. Horn antenna design:

We used a computer program that generated the E-plane [A] and H-plane [B] dimensions given a cutoff frequency (2.4GHz), waveguide standard (WR430), and desired gain (19dB). Once we had the value for A and B, then we used the following equations to designing the horn antenna.

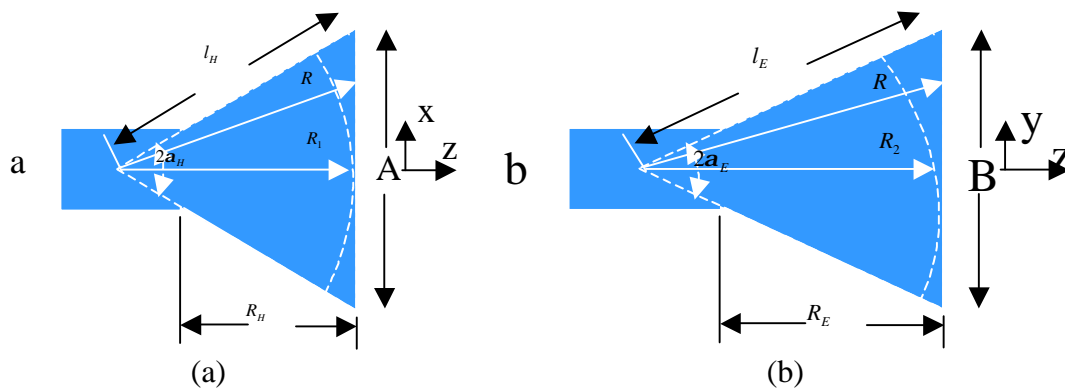


Figure 7: (a) The H-plane and (b) E-plane of the horn antennas.

Horn antenna design was relatively simple. Once you meet the physical constraints of the E and H plane of the aperture then you can use plane geometry and symmetry to get the rest of the dimensions.

Physical constraints:

$$R_1 / R_H = A / (A - a)$$

$$R_2 / R_E = B / (B - b)$$

For optimum horn,

$$B = \frac{1}{2}(b + \sqrt{b^2 + 8IR_E})$$

$$R_E = \frac{A - a}{3I} A$$

$$G = \frac{4p}{I^2} e_{ap} AB = \frac{4p}{I^2} e_{ap} A \frac{1}{2}(b + \sqrt{b^2 + \frac{8A(A-a)}{3}})$$



$$A^4 - aA^3 + \frac{3bGI^2}{8pe_{ap}} A = \frac{3G^2 I^4}{32p^2 e_{ap}^2}$$

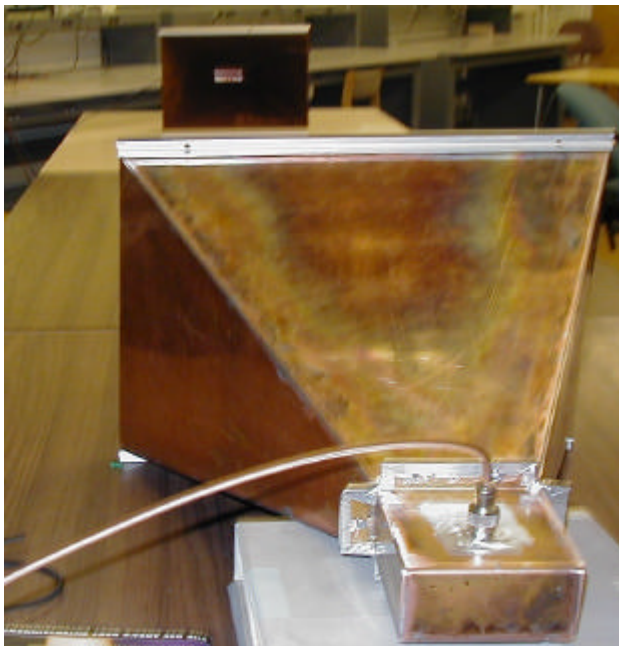
Once each parameter was solved, we fabricated the antennas and the waveguides in the San Jose State University's machine shops in the engineering building. The parameters are shown in table 2.

A [in.]	B [in.]	R _E [in.]	R ₂ [in.]	R ₁ [in.]	l _H [in.]	l _E [in.]
20.50	15.18	22.47	26.19	28.45	30.24	27.27

Table 2: Calculated horn antenna dimensions of each parameter.

III. Test setup and measurements:

The horn antennas were 8 feet apart as shown in picture 4 below. We followed the test methodology we mentioned earlier, and attained the data shown in table 3. Then, radiation pattern shown on figure 8 were plotted.

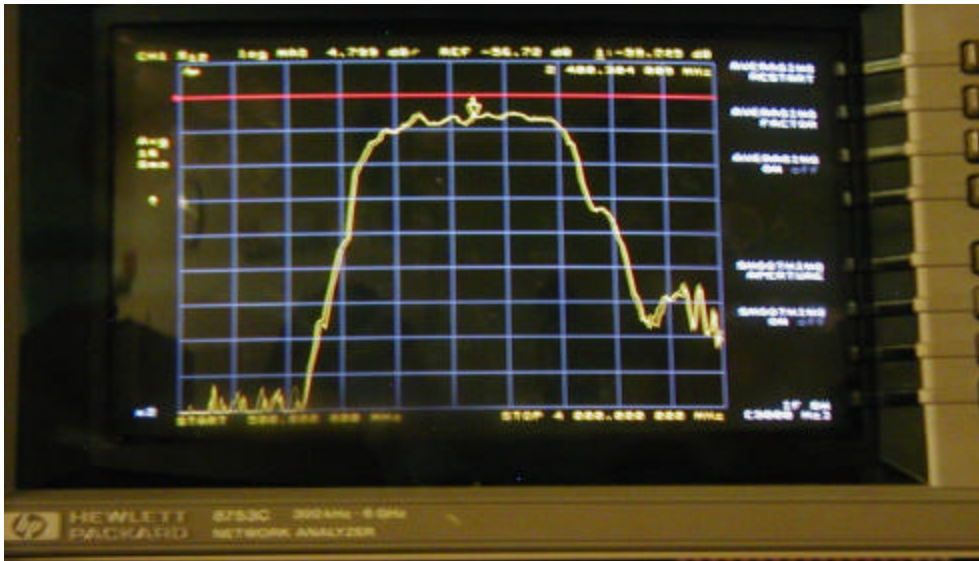


Picture 4: the antenna system setup

The far back antenna is the receiver antenna where we measured S_{21} from and the front antenna is the rotating antenna. The corresponding S_{21} magnetite was changing as we rotated the front antenna. The network analyzer display of S_{12} is shown in picture 5.

Left and Right Rotation			Vertical Rotation
Rotations [Degrees]	S21 [dB] E plane	S21 [dB] H plane	S21[dB] E plane
0	0	-26.6	-35.4
10	-3	-22.1	-37.6
20	-8.85	-19.15	-39.9
30	-17.5	-11.6	-45
40	-23.6	-7.7	-48
50	-35	-0.5	-46.8
60	-37.7	-9.8	-45
70	-39.7	-4.3	-53
80	-51.5	7.8	-63.5
90	-46.5	-1	-75
100	-54	5	
110	-44.6	-4.4	
120	-44.5	-2.2	
130	-42	-7	
140	-43.5	-2	
150	-35.5	-4.3	
160	-31.7	-11.3	
170	-29.3	-15.2	
180	-28	-13.5	
-170	-30.1	-16.3	
-160	-32.5	-12.5	
-150	-36.3	-4.5	
-140	-44.2	-2.3	
-130	-43.1	-8.1	
-120	-44.8	-2.9	
-110	-45	-4.7	
-100	-54	6	
-90	-45	-2	
-80	-52	8	
-70	-41.2	-4.9	
-60	-38.1	-10.1	
-50	-35.3	-0.6	
-40	-23.9	-8.1	
-30	-18.5	-11.7	
-20	-9.1	-20.1	
-10	-3	-23.2	

Table 3: Measured data obtained using a network analyzer.



Picture 5: S_{12} of magnetite as one antenna is rotated while the other is held in place.

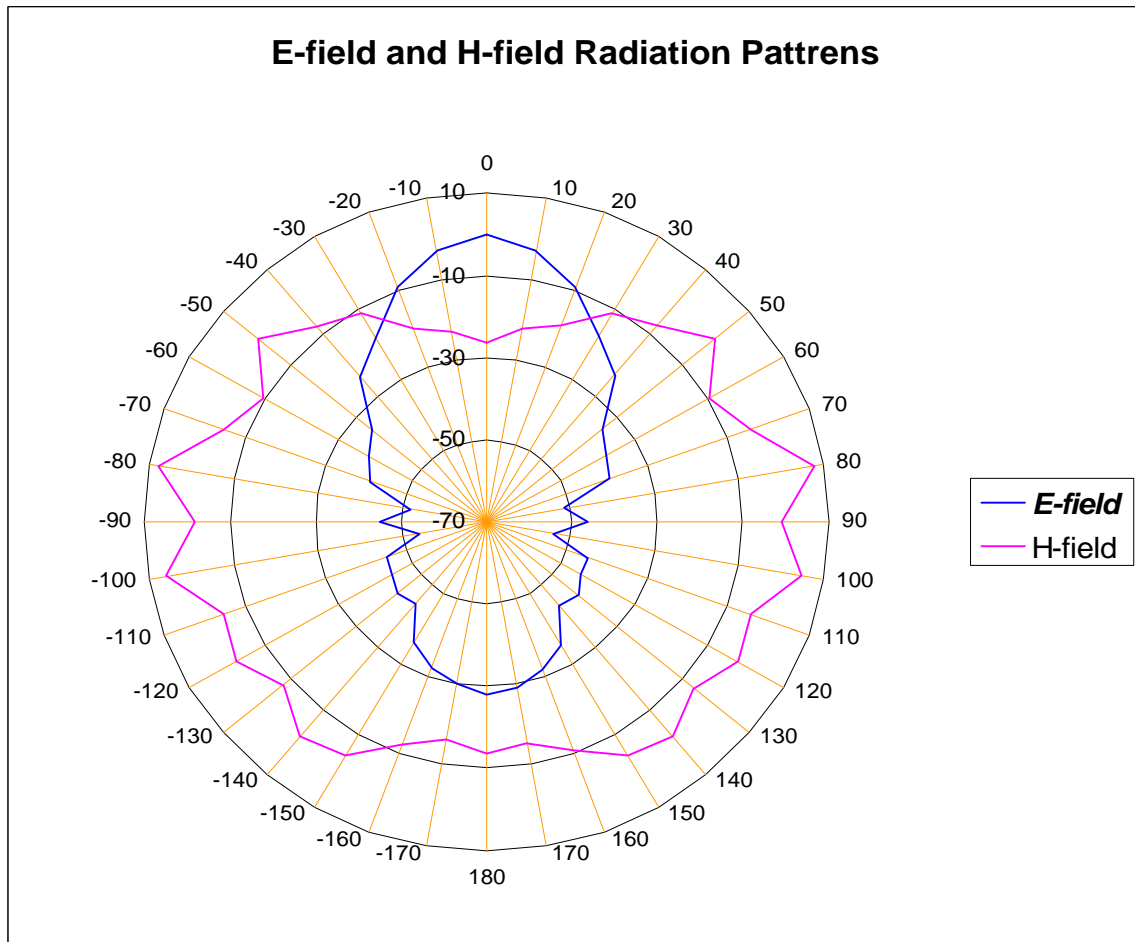


Figure 8: Actual measured E and H field radiation patterns obtained from S_{21} at the receiver end antenna.

Discussion

When comparing the simulated radiation pattern with the actual measured one, one can see significant differences. There are two major reasons for that. The first one is the way the antennas were fabricated. Although we provided the values for each parameter listed in table 2 using the equations mentioned above, the values for l_H and l_E were changed slightly to make the horns fit.

The other problem that contributed to the errors shown in figure 8, where we get radiation when the rotating antenna is more than 110° away from the receiving antenna, is because the test environment was not ideal. The maximum distance (between the two antennas) we had to work with was about 8 feet. The room was full of reflective objects such as metal cabinets, tables, chairs, and the wall.

Concluding remarks

The construction of the horn antennas was simple in terms of paper and pencil. However, fabrication was far more difficult than anticipated before we started the project, but we managed to construct the horn antennas and reach our goal. The resulted measured radiation pattern of the E and H field supports our expected radiation pattern and the calculation of the dimensions of the antennas. Our data could have been improved if we had an adequate antenna testing facility accommodated by a chamber. We tested our antenna in a room full of many objects that were reflecting the radiated signal significantly.

References

1. <http://www.tmeg.com/tutorials/antennas/antennas.htm>
2. <https://ewhdbks.mugu.navy.mil/ANTENNAS.HTM>
3. <http://www.tele.ntnu.no/radio/fag/SIE2080/AntennaLab/AntPatternMeas.pdf>
4. http://www.eecs.umich.edu/emag/labmanual/EECS330_LE9.pdf
5. Tatsuo Itoh, George Haddad, James Harvey, "RF Technologies for Low Power Wireless Communications" IEEE, pp.305-345, John Wiley & Sons, Inc, (2001).
6. Warren L. Stutzman, "Antenna Theory and Design", John Wiley & Sons, (1981)
7. Carr, Joseph J, "Practical Antenna Handbook", TAB BOOKS, (1989).

Appendix

Equations used in simulating the E-Field radiation pattern.

$$F_H(\mathbf{q}) = \frac{1 + \cos \mathbf{q}}{2} \frac{I(\mathbf{q}, \mathbf{f} = 0^0)}{I(\mathbf{q} = 0^0, \mathbf{f} = 0^0)} \quad (1)$$

where

$$I(\mathbf{q}, \mathbf{f} = 0^0) = e^{j\left(\frac{p}{8t}\right)\left[\left(\frac{A}{I}\right)\sin \mathbf{q} + \frac{1}{2}\right]^2} [C(s_2) - jS(s_2) - C(s_1) + jS(s_1)] + e^{j\left(\frac{p}{8t}\right)\left[\left(\frac{A}{I}\right)\sin \mathbf{q} - \frac{1}{2}\right]^2} [C(t_2) - jS(t_2) - C(t_1) + jS(t_1)] \quad (2)$$

where

$$\begin{aligned} s_1 &= 2\sqrt{t} \left[-1 - \frac{1}{4t} \left(\frac{A}{I} \sin \mathbf{q} \right) - \frac{1}{8t} \right] \\ s_2 &= 2\sqrt{t} \left[1 - \frac{1}{4t} \left(\frac{A}{I} \sin \mathbf{q} \right) - \frac{1}{8t} \right] \\ t_1 &= 2\sqrt{t} \left[-1 - \frac{1}{4t} \left(\frac{A}{I} \sin \mathbf{q} \right) + \frac{1}{8t} \right] \\ t_2 &= 2\sqrt{t} \left[1 - \frac{1}{4t} \left(\frac{A}{I} \sin \mathbf{q} \right) + \frac{1}{8t} \right] \end{aligned} \quad (3)$$

$$|F_E(\mathbf{q})| = \frac{1 + \cos \mathbf{q}}{2} \left\{ \frac{[C(r_4) - C(r_3)]^2 + [S(r_4) - S(r_3)]^2}{4[C^2(2\sqrt{s}) + S^2(2\sqrt{s})]} \right\}^{\frac{1}{2}} \quad (4)$$

where

$$s = \frac{B^2}{8IR_2} = \frac{1}{8} \left(\frac{B}{I} \right)^2 \frac{1}{R_2}, \quad t = \frac{A^2}{8IR_1} = \frac{1}{8} \left(\frac{A}{I} \right)^2 \frac{1}{R_1} \quad (5)$$

$$r_3 = 2\sqrt{s} \left[-1 - \frac{1}{4s} \left(\frac{B}{I} \sin \mathbf{q} \right) \right], \quad r_4 = 2\sqrt{s} \left[1 - \frac{1}{4s} \left(\frac{B}{I} \sin \mathbf{q} \right) \right] \quad (6)$$

MatLab Code for simulation

```
lambda = 0.125;
A = 0.5205;
B = 0.3855;
R2 = 0.6652;
a = 0.10922;
b = 0.0546;
b = 0.05461;
R1 = 0.7228;
Rh = 0.571;
t := R1 * Rh;
t = R1 * Rh;
t = A^2;
t = (A^2)/(8*lambda*R1);
s = (B^2)/(8*lambda*R2);
theta = 0:pi/100:2*pi;
s1 = 2*t^(1/2)*(-1-1/(4*t))*((A/lambda)*sin(theta)-1/(8*t));
s2 = 2*t^(1/2)*(1-1/(4*t))*((A/lambda)*sin(theta)-1/(8*t));
t1 = 2*t^(1/2)*(-1-1/(4*t))*((A/lambda)*sin(theta)+1/(8*t));
t2 = 2*t^(1/2)*(1-1/(4*t))*((A/lambda)*sin(theta)+1/(8*t));
Cs2 = quad ('cos(pi/2.*(x.^2))', s2, 0);
Cs1 = quad ('cos(pi/2.*(x.^2))', s1, 0);
Ct2 = quad ('cos(pi/2.*(x.^2))', t2, 0);
Ct1 = quad ('cos(pi/2.*(x.^2))', t1, 0);
Ss2 = quad ('sin(pi/2.*(x.^2))', s2, 0);
Ss1 = quad ('sin(pi/2.*(x.^2))', s1, 0);
St1 = quad ('sin(pi/2.*(x.^2))', t1, 0);
St2 = quad ('sin(pi/2.*(x.^2))', t2, 0);
r3 = 2*s^(1/2)*(-1-1/(4*s))*((B/lambda)*sin(theta));
r4 = 2*s^(1/2)*(1-1/(4*s))*((B/lambda)*sin(theta));
Cr4 = quad ('cos(pi/2.*(x.^2))', r4, 0);
Cr3 = quad ('cos(pi/2.*(x.^2))', r3, 0);
C2sqrs = quad ('cos(pi/2.*(x.^2))', 2*s^(1/2), 0);
Sr4 = quad ('sin(pi/2.*(x.^2))', r4, 0);
Sr3 = quad ('sin(pi/2.*(x.^2))', r3, 0);
S2sqrs = quad ('sin(pi/2.*(x.^2))', 2*s^(1/2), 0);
Iphi0 =
exp(j*(pi/8*t))*((A/lambda)*sin(theta)+1/2).^2.*(Cs2-j*Ss2-Cs1+j*Ss1)+
exp(j*(pi/8*t))*((A/lambda)*sin(theta)-1/2).^2.*(Ct2-j*St2-Ct1+j*St1);

Iphi0zero =
exp(j*(pi/8*t))*((A/lambda)*sin(0)+1/2).^2.*(Cs2-j*Ss2-Cs1+j*Ss1)+
exp(j*(pi/8*t))*((A/lambda)*sin(0)-1/2).^2.*(Ct2-j*St2-Ct1+j*St1);

Fhtheta = (1+cos(theta))/2 * (Iphi0/Iphi0zero);

Fetheta = (1+cos(theta))/2 .* (((Cr4-Cr3).^2 +
(Sr4-Sr3).^2)./(4*((C2sqrs.^2)+(S2sqrs.^2)))).^(1/2)
polar(theta, Fhtheta, '--r');
hold on;
polar(theta, Fetheta, '--o');
```